

1-1-2010

Kinetics of the Hydrogen Electrode Reaction

Saurabh A. Vilekar

Ilie Fishtik

Worcester Polytechnic Institute, ifishtik@wpi.edu

Ravindra Datta

Worcester Polytechnic Institute, rdatta@wpi.edu

Follow this and additional works at: <http://digitalcommons.wpi.edu/chemicalengineering-pubs>



Part of the [Chemical Engineering Commons](#)

Suggested Citation

Vilekar, Saurabh A. , Fishtik, Ilie , Datta, Ravindra (2010). Kinetics of the Hydrogen Electrode Reaction. *Journal of the Electrochemical Society*, 157(7), B1040-B1050.

Retrieved from: <http://digitalcommons.wpi.edu/chemicalengineering-pubs/25>

This Article is brought to you for free and open access by the Department of Chemical Engineering at DigitalCommons@WPI. It has been accepted for inclusion in Chemical Engineering Faculty Publications by an authorized administrator of DigitalCommons@WPI.



Kinetics of the Hydrogen Electrode Reaction

Saurabh A. Vilekar,* Ilie Fishtik, and Ravindra Datta^z

Fuel Cell Center, Department of Chemical Engineering, Worcester Polytechnic Institute, Worcester, Massachusetts 01609, USA

It is well recognized that the standard Butler–Volmer equation is lacking in an adequate description of the kinetics of the hydrogen electrode reaction over the complete range of potentials for the alkaline as well as the acid electrolytes. Further, it is unable to explain the asymmetry in current vs potential observed in the hydrogen evolution reaction (HER) vs the hydrogen oxidation reaction (HOR). In fact, even kinetic descriptions via two-step mechanisms (Volmer–Heyrovsky, Volmer–Tafel, or Heyrovsky–Tafel) are individually applicable only in limited potential ranges. We present an approach that provides explicit rate expressions involving kinetics of all the three steps (Tafel–Volmer–Heyrovsky) simultaneously, as well as more limiting rate expressions based on two-step pathways. The analysis is based on our recently developed graph–theoretic approach that provides accurate rate laws by exploiting the electrical analogy of the reaction network. The accuracy of the resulting rate expressions, as well as their asymmetric potential dependence, for both HOR and HER is illustrated here based on step kinetics provided in the literature for Pt catalyst in 0.5 M NaOH solution.

© 2010 The Electrochemical Society. [DOI: 10.1149/1.3385391] All rights reserved.

Manuscript submitted January 11, 2010; revised manuscript received March 16, 2010. Published May 21, 2010.

Due to their practical significance, the hydrogen oxidation reaction (HOR) and its reverse, i.e., the hydrogen evolution reaction (HER), are by far the most extensively investigated of electrocatalytic reactions.^{1–8} Further, despite being among the simplest of such reactions, their mechanistic and kinetic understanding is still incomplete. The significance of dual-pathway kinetics has recently been shown for the HOR on Pt electrode.⁷ However, no general rate expression exists that can simultaneously account for these alternate pathways in terms of the accepted three-step mechanism, namely, the Tafel, Volmer, and the Heyrovsky steps. Further, no realistic first-principles prediction of step kinetics yet exists for the hydrogen electrode reaction, although there is now great interest in *ab initio* predictions^{9–16} as well as in their experimental validation.^{5,8,12,17–22} Were an accurate rate expression for HOR/HER in terms of its three-step kinetics available, it would not only be revealing, allowing fundamental questions to be answered, such as those posed recently by Gasteiger et al.,²² but when available, it could utilize the first-principles predictions of step kinetics to construct a comprehensive picture of this important and intriguing reaction system, including the elucidation of parallel pathways and the dominant steps. A thorough understanding of HOR and HER would also serve as a yardstick for understanding other electrocatalytic reactions.

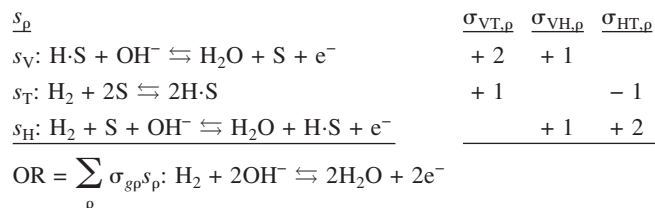
Following up on our earlier work,³ we present here a detailed analysis of the hydrogen electrode reaction based on a graph–theoretic approach we recently developed, namely, the reaction route (RR) graph approach.^{3,23–27} It involves a topological analysis of alternate pathways as walks on the RR graph, coupled with a kinetic analysis based on Kirchhoff’s laws of (*i*) flux (i.e., mass conservation) at nodes interconnecting reaction steps represented as branches or edges and of (*ii*) potential (i.e., state property of thermodynamic potentials) applicable to cycles among mechanistic steps in the RR graph. This procedure is completely analogous to electric circuit analysis, thus allowing the direct use of the electrical analogy in kinetic analysis. Although our earlier work was limited to numerical analysis,³ here we exploit the electrical analogy to provide explicit rate expressions. The results presented below confirm the importance of two dominant two-step pathways on Pt electrode in alkaline media at different electrode potentials. Further, the complete rate expression provided here that involves all the three mechanistic steps, namely, the Tafel, Volmer, and Heyrovsky steps, is needed for an adequate description over the complete range of potentials of interest for HER and HOR.

Our methodology to deduce a steady-state rate expression for the hydrogen electrode reaction is, thus, based on the RR graph and its

electrical analog, along with the notion of intermediate reactions (IRs) for the formation of an intermediate species. It further interrelates the two standard approaches of kinetic analysis, namely, the rate-determining step (RDS)/quasi-equilibrium (QE) approach of Langmuir–Hinshelwood–Hougen–Watson (LHHW)²⁸ and the quasi-steady-state (QSS) analysis of Bodenstein.^{29–32} The resulting rate expression accurately portrays the kinetics of HOR/HER over a broad range of potentials, including their asymmetric potential dependence in both alkaline and acidic media, although in the discussion below we simply use the step rate constants reported for Pt in an alkaline electrolyte. The case of acidic electrolyte, of special interest in fuel cells, will be described in a subsequent publication.

Reaction Mechanism, Network, and Step Kinetics

RRs or pathways.— The hydrogen electrode reaction has been investigated over a long period of time due to its technological and fundamental significance. The most common and well-accepted mechanism involves the Tafel, Volmer, Heyrovsky steps,^{33–35} which have adequately explained the overall reaction (OR) kinetics.^{7,12,13,16,36} This three-step mechanism involves only a single reaction intermediate, H·S, where S represents an unoccupied catalyst surface site. However, more recently, other intermediates have been proposed. For instance, intermediates such as adsorbed water (H₂O·S) and adsorbed hydroxyl (OH·S) have been shown to exist on Pt surfaces by Völkening et al.,³⁷ Bedürftig et al.,³⁸ and Rossmel et al.³⁹ Thus, Nørskov et al.¹³ consider the OH·S and O·S species to calculate the effect of molecular water on adsorption. Additional intermediates, of course, imply additional elementary steps in the mechanism and would alter the site balance. Nonetheless, because our purpose here is to elucidate an approach that adequately describes the kinetics of the hydrogen electrode reaction, we simply adopt the standard Tafel–Volmer–Heyrovsky mechanism shown below to avoid being distracted by the additional complexities of a more detailed mechanism, which are left for future work

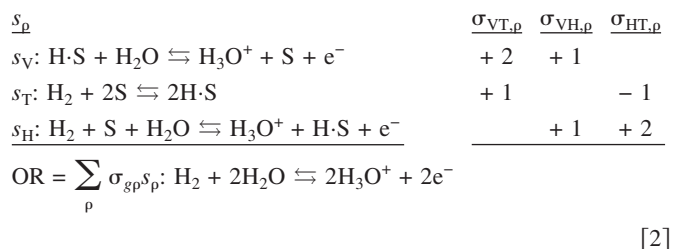


[1]

Equation 1 above describes the HOR in an alkaline electrolyte. In an acidic electrolyte, however, the corresponding mechanism is

* Electrochemical Society Student Member.

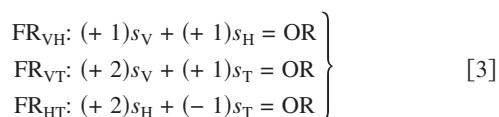
^z E-mail: rdatta@wpi.edu



The Volmer step, s_V , above describes the electrochemical consumption of the key intermediate, namely, the surface atomic hydrogen, H·S, whereas the nonelectrochemical Tafel step, s_T , and the electrochemical Heyrovsky step, s_H , describe the generation of H·S from molecular H_2 . As indicated by the stoichiometric numbers $\sigma_{g\rho}$ above, when these steps are combined in a manner that eliminates the intermediate H·S, the OR results. Clearly, this can be accomplished in more than one way, which represents the alternate RRs or pathways. The OR and the elementary steps for the HER are simply the reverse of those written above for the HOR.

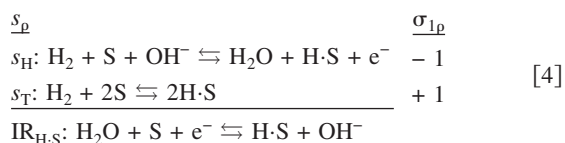
More generally, the OR results from a linear combination of the elementary steps s_{ρ} ($\rho = 1, 2, \dots, p$) in a mechanism, i.e., $\sum_{\rho=1}^p \sigma_{g\rho} s_{\rho} = \text{OR}$, representing the g th RR, wherein all the intermediate species I_k ($k = 0, 1, 2, \dots, q$) are eliminated to provide the OR in terms of only the terminal species T_i ($i = 1, 2, \dots, n$), i.e., the reactants and products of the OR. Here, $\sigma_{g\rho}$ is the stoichiometric number (usually, 0, ± 1 , or ± 2) of step s_{ρ} in the g th RR.

The RRs that produce the OR are, in fact, referred to more specifically as full routes (FRs). Thus, as shown in Eq. 1 and 2, the three FRs for the HOR are



The FR_{VH} represents the Volmer–Heyrovsky pathway, whereas FR_{VT} and FR_{HT} are the Volmer–Tafel and the Heyrovsky–Tafel pathways, respectively. A negative stoichiometric number, as shown above, simply means that the step in the given RR is followed in the reverse direction to that indicated in the mechanism. Because all elementary steps are reversible, in principle, although the degree of reversibility of a step, $z_{\rho} \equiv \tilde{r}_{\rho}/\bar{r}_{\rho}$, may vary widely, this does not present a problem.

Other linear combinations or RRs that do not eliminate all of the intermediate species and produce the so-called IRs are called intermediate reaction routes (IRRs). For example, $(-1)s_H + (+1)s_T = \text{IR}$, that is



which is an intermediate reaction that describes the formation of an intermediate, namely, H·S from the terminal species water and electron, as well as the vacant sites, S. We will discuss IRs further later on.

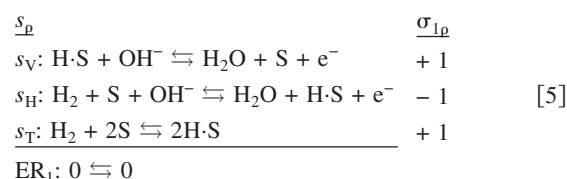
More generally, we define an IRR as a linear combination, $\sum_{\text{IR}_k} \sigma_{kj} s_j = \text{IR}_k$, in which all the intermediate species except the one of interest I_k (along with a reference intermediate, say surface site, S) are eliminated.^{40,41} The IRs produced by these IRRs may be written generally as, $\text{IR}_k: \gamma_k I_k + (-\gamma_k)S + \sum_{i=1}^n (\gamma_{ki})T_i = 0$, where γ_k is positive because the intermediate I_k is considered as a product in the IR.

Further, there are other RRs or linear combination of steps that eliminate all of the species, both intermediate and terminal. Such RRs are called empty routes (ERs) or cycles, as they produce a “zero” OR (i.e., the stoichiometric coefficients of all the species are

Table I. Stoichiometrically distinct direct FRs and ERs for the three-step HER mechanism.

RR	Expression
Full RRs	
FR_{VH} (Volmer–Heyrovsky):	$s_V + s_H = \text{OR}$
FR_{VT} (Volmer–Tafel):	$2s_V + s_T = \text{OR}$
FR_{HT} (Heyrovsky–Tafel):	$2s_H - s_T = \text{OR}$
Empty RRs	
ER_1 :	$s_V - s_H + s_T = 0$

zero). In fact, because subtracting one FR from the other, e.g., $\text{FR}_{VT} - \text{FR}_{VH}$, would eliminate all species, it can provide an ER, namely, $(+1)s_V + (-1)s_H + (+1)s_T = 0$, is an ER, ER_1



In general, thus, $\text{ER}_g: \sum_{\rho=1}^p \sigma_{g\rho} s_{\rho} = 0$ represents an ER.

Finally, let us consider another linear combination of FRs, e.g., $\text{FR}_{VT} + \text{FR}_{VH} - \text{FR}_{HT}$, which simply results in another FR, namely, $\text{FR}_g: (+3)s_V + (+2)s_T + (-1)s_H = \text{OR}$. In fact, because new RRs may be obtained simply by linearly combining others, one may, in principle, obtain an infinite set, if no further restrictions are placed on their definition.

This is avoided by the concept of “directness” proposed by Milner,⁴² i.e., the number of steps involved in an RR must be minimal. In other words, a “direct” FR must not contain any cycles or ERs. Such a direct FR contains no more than $q + 1$ steps, whereas a direct ER contains no more than $q + 2$ steps.^{23,24,26} selected from among the given mechanism of p steps. Here, q is the number of linearly independent intermediate species, typically 1 less than the number of intermediates due to intermediates conservation, e.g., site conservation. For the three-step ($p = 3$) HOR/HER reaction mechanism considered here, H·S is, in fact, the only independent intermediate, so that $q = 1$ simply.

For the hydrogen electrode reaction, thus, a direct FR must not contain more than any two of the three steps, whereas a direct ER must be restricted to less than three steps. As a result, the FR obtained above from the combination of others, i.e., $\text{FR}_g: (+3)s_V + (+2)s_T + (-1)s_H = \text{OR}$ is not an appropriate FR as it contains three elementary steps. In fact, it has embedded in it a cycle, namely, $\text{ER}_1: (+1)s_V + (-1)s_H + (+1)s_T = 0$, which if subtracted from it, results in FR_{VT} .

With this restriction on path length, a finite and unique set of FRs and ERs results, as listed in Table I for the above HOR/HER mechanism. As per the Horiuti–Temkin theorem, furthermore, an independent RR set is any set of $\mu = p - q = 3 - 1 = 2$ RRs, which may include both FRs and ERs, so long as they include among them all of the steps in the mechanism. Moreover, the number of linearly independent ERs is given by $p - (q + 1) = 3 - 2 - 1 = 1$ for the reaction mechanism considered.²³ Thus, a set of two linearly independent RRs may be readily determined by identifying one independent ER and one FR by a simple inspection of the HER/HOR mechanism, as done above, thus avoiding the stoichiometric enumeration of RRs used for complex mechanisms.^{23,24,26} Let us consider the FR_{VH} and ER_1 , mentioned above as the independent set of RRs for the considered HOR/HER mechanism, from which the remaining set of unique RRs can be obtained. Thus, a linear combination of FR_{VH} and ER_1 results in FR_{VT} and FR_{HT} (Table I).

These RRs or pathways may, in fact, be simply traced as walks on the RR graph of a mechanism for an OR. The construction of

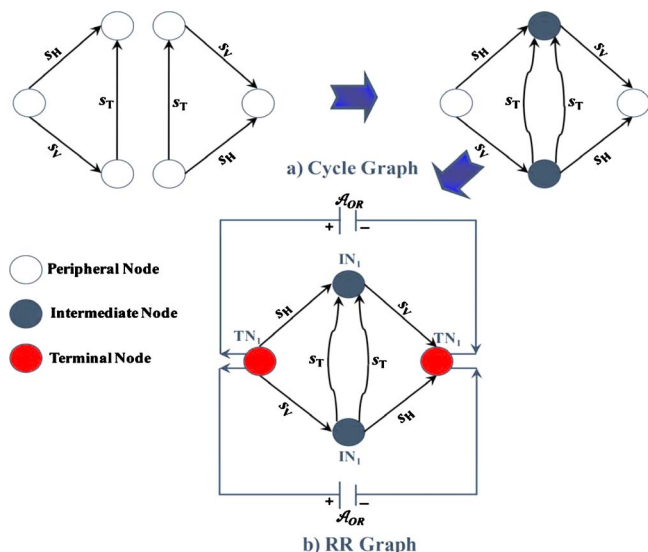


Figure 1. (Color online) RR graph construction for the three-step HER mechanism.

such a graph is discussed in detail by us elsewhere^{23,24,26} and is described below briefly with regard to the hydrogen electrode reaction, as done elsewhere.³

RR graph.— An RR graph is a graph-theoretical depiction of the mechanism of an OR, in which the elementary steps are represented individually by directed branches or edges, interconnected at nodes or vertices, such that all possible RRs enumerable, for instance, from stoichiometric considerations,^{23,24,26,43} can be traced on it simply as walks between terminal nodes (TNs) across which the OR is connected. These RR graphs further follow Kirchhoff's laws of flow graphs rooted in the species conservation principle along with the state property of thermodynamic functions, which provide the topological constraints on the individual step rates. Of course, Kirchhoff's laws are central to the analysis of electrical networks. For this reason, RR graphs are completely analogous to electrical networks. In fact, a QSS rate expression of Ohm's law form, i.e., OR rate = driving force/overall network resistance, can be derived by exploiting the analogy to electrical circuits. This property is used below to obtain a general rate law for the kinetics of HOR/HER.

With the independent set of RRs (i.e., FR_{VH} and ER_1) at hand, the construction of the RR graph is straightforward and is illustrated in Fig. 1.³ We start by assembling the ERs, only ER_1 in this case, into a cycle graph. It is further noted that there exists nonunit stoichiometric ($\sigma_{gp} = +2$) numbers in some of the RRs in the unique set (Table I), i.e., in FR_{VT} and in FR_{HT} . This implies that every elementary reaction step s_p as well as the OR must occur twice in the RR graph, which must furthermore be symmetrical.^{26,27} This can be accomplished by fusing two ER_1 s, as shown in Fig. 1a. Next, the remaining RR of the independent set, namely, FR_{VH} , can be included in the graph by simply connecting the OR (also twice) across TNs, yielding the final RR graph (Fig. 1b). All of the four unique RRs (Table I) for HOR can be traced on the resulting RR graph as walks between the TNs. In fact, every RR in the graph is involved twice. This is a consequence of the fact that the mechanism is nonminimal,²⁶ i.e., the elementary steps are involved more than once in a FR. Nonetheless, the affinity (or any other thermodynamic potential change across it) and the rate of a step (e.g., s_H , s_V , or s_T) remain unchanged regardless of their placement because of the network symmetry. For HER, the FR walks are simply in the opposite direction.

The other characteristic that an appropriate RR graph must satisfy is that the connectivity at the intermediate nodes (INs) and the TNs must be consistent with the QSS condition for the intermediate

and terminal species. Thus, INs interconnect mechanistic steps s_p only, with the incidence of steps being consistent with the QSS conditions for intermediates or their linear combination, along with the condition of minimality. The TNs, however, interconnect mechanistic steps s_p to the OR, with the incidence of steps being consistent with QSS equations for terminal species as well as with minimality of incidence.^{23,24,26}

Because there is only one linearly independent intermediate here, H-S, its QSS condition is

$$Q_{H-S}: (-2)r_T + (+1)r_V + (-1)r_H = 0 \quad [6]$$

which is consistent with the connectivity, $\sum_p m_{pj}s_p = 0$, where the incidence coefficient $m_{pj} = +1$, if a branch leaves the node j , and $m_{pj} = -1$, if a branch is coming into the node j , of the only one IN (although present twice) in the RR Graph, that is

$$IN_1: (-2)s_T + (+1)s_V + (-1)s_H = 0 \quad [7]$$

Similarly, the QSS condition for the terminal species (H_2, OH^-, H_2O, e^-) for the HOR in alkaline electrolyte (Eq. 1) are

$$\left. \begin{aligned} Q_{H_2}: (-1)r_{OR} + (-1)r_T + (-1)r_H &= 0 \\ Q_{H_2O}: (+2)r_{OR} + (+1)r_V + (+1)r_H &= 0 \\ Q_{e^-}: (+2)r_{OR} + (+1)r_V + (+1)r_H &= 0 \\ Q_{OH^-}: (-2)r_{OR} + (-1)r_V + (-1)r_H &= 0 \end{aligned} \right\} \quad [8]$$

The QSS condition for OH^- , e^- , and H_2O is the same and is represented by the TN_1 (represented twice) in the RR graph, namely

$$TN_1: 2OR - s_V - s_H = 0 \quad [9]$$

Thus, the resulting RR graph satisfies all of the conditions imposed on the RR graph, i.e., all nodes are balanced in that they satisfy the QSS conditions of one or more surface intermediates (in case of INs) and of one or more terminal species (in case of TNs). Further, all the RRs can be traced as walks or paths on the RR graph. The network includes the commonly considered Volmer–Heyrovsky and Volmer–Tafel pathways, along with the not so common Heyrovsky–Tafel pathway.³ Thus, this is an appropriate RR graph for the hydrogen electrode reaction.

Finally, a curious observation by Gennero de Chialvo and Chialvo^{12,36} that two distinct sets of alternate parameters provide identical HOR/HER kinetics can be explained simply from the topology of the RR graph. Thus, it is clear from the symmetry of the RR graph in Fig. 1b that the Volmer and the Heyrovsky steps can be interchanged without affecting the properties of the circuit. As a result, interchanging the kinetic parameters of the Volmer and the Heyrovsky steps does not alter the current density vs overpotential predictions, as found by Gennero de Chialvo and Chialvo,^{12,36} even though it changes the dependence of surface coverage on η from $\theta_{H-S}(\eta)$ to $1 - \theta_{H-S}(\eta)$.

We will use the RR graph in Fig. 1b below for deriving a QSS rate law based on its electrical analog, which would include the flux along all the three pathways (FRs), so that one need not select a pathway individually for kinetic analysis, as is the usual practice. Earlier, we had used this RR graph for a numerical QSS kinetic analysis.³

Step kinetics.— The net rate of a generic elementary step, $r_p = \vec{r}_p - \bar{r}_p$, may be written as

Table II. Reaction rate constants for HER on Pt in 0.5M NaOH at 296 K.³⁶

Reaction step, s_ρ	\tilde{k}_{ρ,Φ_0} (mol cm ⁻² s ⁻¹)	\tilde{k}_{ρ,Φ_0} (mol cm ⁻² s ⁻¹)
$s_T: \text{H}_2 + 2\text{S} \rightleftharpoons 2\text{H}\cdot\text{S}$	$\tilde{k}_T = 8.8 \times 10^{-10}$	$\tilde{k}_T = 8.8 \times 10^{-8}$
$s_V: \text{H}\cdot\text{S} + \text{OH}^- \rightleftharpoons \text{H}_2\text{O} + \text{S} + \text{e}^-$	$\tilde{k}_{V,\Phi_0} = 4.4 \times 10^{-7}$	$\tilde{k}_{V,\Phi_0} = 4.4 \times 10^{-8}$
$s_H: \text{H}_2 + \text{S} + \text{OH}^- \rightleftharpoons \text{H}_2\text{O} + \text{H}\cdot\text{S} + \text{e}^-$	$\tilde{k}_{H,\Phi_0} = 2.4 \times 10^{-10}$	$\tilde{k}_{H,\Phi_0} = 2.4 \times 10^{-9}$

$$\begin{aligned} \tilde{r}_\rho &= \tilde{k}_\rho \prod_{i=1}^n a_i^{-\tilde{\nu}_{\rho i}} \prod_{k=0}^q \theta_k^{-\tilde{\alpha}_{\rho k}} = \tilde{\omega}_\rho \prod_{k=0}^q \theta_k^{-\tilde{\alpha}_{\rho k}} \\ \tilde{r}_\rho &= \tilde{k}_\rho \prod_{i=1}^n a_i^{\tilde{\nu}_{\rho i}} \prod_{k=0}^q \theta_k^{\tilde{\alpha}_{\rho k}} = \tilde{\omega}_\rho \prod_{k=0}^q \theta_k^{\tilde{\alpha}_{\rho k}} \end{aligned} \quad [10]$$

where θ_k is the (unknown) activity of intermediate species I_k ($k = 0, 1, 2, \dots, q$), a_i is the (known or specified) activity of terminal species T_i ($i = 1, 2, \dots, n$), $\tilde{\alpha}_{\rho k}$ is the stoichiometric coefficient of I_k in reaction step s_ρ as a reactant and that as a product is $\tilde{\alpha}_{\rho k}$, whereas that for T_i is $\tilde{\nu}_{\rho i}$ and $\tilde{\nu}_{\rho i}$, respectively. It is, further, useful to club together, in the above mass-action kinetics, the product of the known rate parameters and activities of terminal species into reaction weights, $\tilde{\omega}_\rho$, leaving behind the rates explicitly in terms of the unknown intermediates concentrations and known $\tilde{\omega}_\rho$.

The thermodynamic transition-state theory gives the rate constants of the forward and reverse steps as⁴⁴

$$\tilde{k}_\rho \equiv \kappa \frac{k_B T}{h} \exp\left(-\frac{\Delta \tilde{G}_\rho^{\ddagger,0}}{RT}\right) \quad \tilde{k}_\rho \equiv \kappa \frac{k_B T}{h} \exp\left(-\frac{\Delta \tilde{G}_\rho^{\ddagger,0}}{RT}\right) \quad [11]$$

where the Gibbs free energy of activation involves electrostatic potential as well, $\Delta \tilde{G}_\rho^{\ddagger,0} = \Delta \tilde{G}_\rho^{\ddagger,0} - \beta_\rho (\nu_{\rho e} F \Phi)$, as per the linear free energy relation. Further, use of the relation $\Delta \tilde{G}_\rho^{\ddagger,0} = \Delta \tilde{H}_\rho^{\ddagger,0} - T \Delta \tilde{S}_\rho^{\ddagger,0}$ provides, e.g., the forward rate constant as

$$\begin{aligned} \tilde{k}_\rho &= \underbrace{\kappa \frac{k_B T}{h} \exp\left(\frac{\Delta \tilde{S}_\rho^{\ddagger,0}}{R}\right)}_{\tilde{\Lambda}_\rho} \exp\left(-\frac{\Delta \tilde{H}_\rho^{\ddagger,0}}{RT}\right) \exp\left\{\frac{(\beta_\rho) \nu_{\rho e} F \Phi}{RT}\right\} \\ &= \tilde{\Lambda}_\rho \exp\left(-\frac{\tilde{E}_{\rho,\Phi=0}}{RT}\right) \exp\left\{\frac{(\beta_\rho) \nu_{\rho e} F \Phi}{RT}\right\} \\ &= \tilde{k}_{\rho,\Phi_0} \exp\left\{\frac{(\beta_\rho) \nu_{\rho e} F \eta_\rho}{RT}\right\} \end{aligned} \quad [12]$$

where the symmetry factor is assumed to be $\beta_\rho = 1/2$ for an elementary reaction, \tilde{k}_{ρ,Φ_0} is the rate constant corresponding to equilibrium electrode potential Φ_0 , and $\eta_\rho \equiv \Phi - \Phi_0$ is the overpotential potential. The ‘‘standard’’ (for unit activities) electrode potentials (denoted by superscript o) for the hydrogen electrode reaction are, of course, $\Phi_0^o = 0.000$ V for acidic electrolytes and $\Phi_0^o = -0.828$ V for alkaline electrolytes. Further, \tilde{k}_{ρ,Φ_0} and \tilde{k}_{ρ,Φ_0} in the above are rate constants corresponding to equilibrium electrode potential Φ_0 , that is

$$\tilde{k}_{\rho,\Phi_0} = \tilde{\Lambda}_\rho \exp\left(-\frac{\tilde{E}_{\rho,\Phi=0}}{RT}\right) \exp\left[\frac{(\beta_\rho) \nu_{\rho e} F \Phi_0}{RT}\right] \quad [13]$$

and

$$\tilde{k}_{\rho,\Phi_0} = \tilde{\Lambda}_\rho \exp\left(-\frac{\tilde{E}_{\rho,\Phi=0}}{RT}\right) \exp\left[\frac{(\beta_\rho - 1) \nu_{\rho e} F \Phi_0}{RT}\right] \quad [14]$$

This clearly shows the nature of the pre-exponential factor, $\tilde{\Lambda}_\rho = \kappa (k_B T/h) \exp(\Delta \tilde{S}_\rho^{\ddagger,0}/R)$, the activation energy that explains the temperature dependence in the usual Arrhenius form with the activation energy being related to the enthalpy of activation in the absence of potential, $\tilde{E}_{\rho,\Phi=0} = \Delta \tilde{H}_\rho^{\ddagger,0}$, and the potential dependence via the usual Butler–Volmer form. Clearly, both temperature and potential have a substantial effect on the rate constant of an electrochemical step. However, for the nonelectrochemical steps, e.g., the Tafel step, the potential dependence is clearly zero, and the rate constant simplifies to the Arrhenius expression, $\tilde{k}_\rho = \tilde{\Lambda}_\rho \exp(-\tilde{E}_{\rho,\Phi=0}/RT)$. It should further be apparent that the pre-exponential factor is the same for both chemical and nonelectrochemical steps. Further, any conclusions about the RDS, and the importance of the different pathways, etc., are temperature- as well as potential-dependent.

Thus, the net rates, $r_\rho = \tilde{r}_\rho - \tilde{r}_\rho$, of the three elementary steps in the HOR/HER mechanism may be written as

$$\begin{cases} r_T = \tilde{\omega}_T (1 - \theta_{\text{H}\cdot\text{S}})^2 - \tilde{\omega}_T \theta_{\text{H}\cdot\text{S}}^2 \\ r_V = \tilde{\omega}_V \theta_{\text{H}\cdot\text{S}} - \tilde{\omega}_V (1 - \theta_{\text{H}\cdot\text{S}}) \\ r_H = \tilde{\omega}_H (1 - \theta_{\text{H}\cdot\text{S}}) - \tilde{\omega}_H \theta_{\text{H}\cdot\text{S}} \end{cases} \quad [15]$$

where the site balance, namely, $\theta_0 + \theta_{\text{H}\cdot\text{S}} = 1$, has been incorporated.

The step weights in the above may be written as

$$\begin{aligned} \tilde{\omega}_T &= \tilde{k}_T a_{\text{H}_2} & \tilde{\omega}_T &= \tilde{k}_T \\ \tilde{\omega}_V &= \tilde{\omega}_{V,0} e^\psi & \tilde{\omega}_V &= \tilde{\omega}_{V,0} e^{-\psi} \\ \tilde{\omega}_H &= \tilde{\omega}_{H,0} e^\psi & \tilde{\omega}_H &= \tilde{\omega}_{H,0} e^{-\psi} \end{aligned} \quad [16]$$

where the dimensionless electrode overpotential, $\psi \equiv (1/2) \times (F \eta / RT)$. Further, for the alkaline electrolytes, the parameters above, in terms of the rate constants at equilibrium electrode potential and the activities of the terminal species, are

$$\begin{aligned} \tilde{\omega}_{V,0} &= \tilde{k}_{V,\Phi_0} a_{\text{OH}^-} & \tilde{\omega}_{V,0} &= \tilde{k}_{V,\Phi_0} a_{\text{H}_2\text{O}} \\ \tilde{\omega}_{H,0} &= \tilde{k}_{H,\Phi_0} a_{\text{OH}^-} a_{\text{H}_2} & \tilde{\omega}_{H,0} &= \tilde{k}_{H,\Phi_0} a_{\text{H}_2\text{O}} \end{aligned} \quad [17]$$

Furthermore, in these expressions, the activity of water is usually assumed to be unity, i.e., $a_{\text{H}_2\text{O}} = 1$, for saturated conditions, whereas the activity of hydrogen is written as its partial pressure, i.e., $a_{\text{H}_2} = p_{\text{H}_2}$, in atm.

Unfortunately, the rate constants for electrocatalytic elementary reactions are not yet available from first-principles predictions, although important progress is being made in this direction.^{9-11,15,16} Therefore, for our analysis, we adopt rate constants obtained in the literature by fitting experimental rate data. Thus, the set of rate constants used here for the Pt catalyst in 0.5 M NaOH solution at 296 K is provided in Table II.^{36,45} The kinetic analysis given below is,

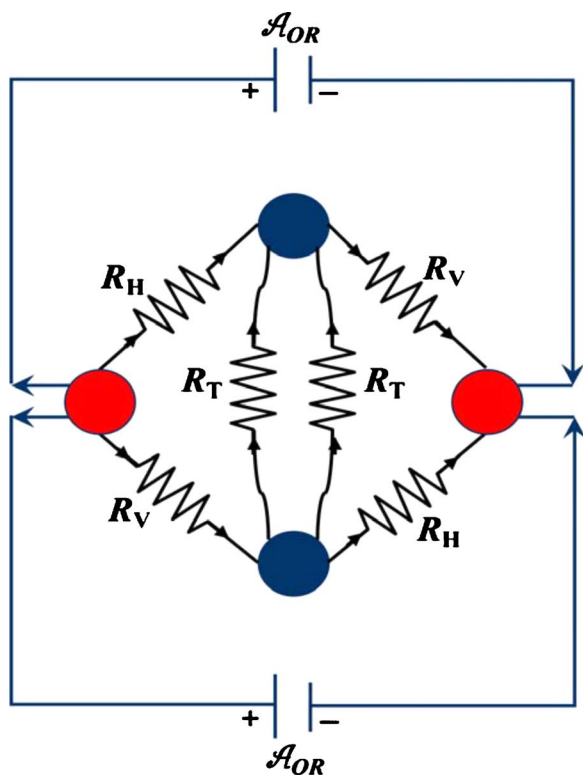


Figure 2. (Color online) The equivalent electrical circuit for the three-step HER mechanism.

however, independent of the HOR/HER conducted in alkaline or acid electrolyte and how the rate constants might have been obtained.

Kinetic Analysis via Kirchhoff's Network Laws

The electrical analogy.— Any quantitative network involving flow (e.g., reaction network or a piping network) must be consistent with two basic laws (Kirchhoff's laws) of networks, i.e., (i) consistency with conservation principle (e.g., of mass) at the nodes along with (ii) the thermodynamic constraint, i.e., path independence of thermodynamic potentials, e.g., pressure drop in a piping system. As another example, Gibbs free energy, or enthalpy or entropy change over the network elements of a process graph must add up to that of the overall process, and it must be zero for a cycle. Thus, the corresponding laws in electrical networks are Kirchhoff's current law (charge balance at nodes) and Kirchhoff's voltage law (voltage drops add up to zero in a cycle).

Further, because the use of these network laws is well ingrained in the electrical circuit analysis, it is conceptually useful, although not essential, to draw an analogy of the RR graphs to electrical networks. In fact, an RR graph can be directly converted into an equivalent electric circuit,^{3,23,24,26,27} thus facilitating its analysis by allowing use of the vast array of techniques available for electric circuit analysis.⁴⁶ Thus, each branch in the RR graph may be replaced by its equivalent impedance, or "resistance" R_p , for the steady-state analysis, whereas the branch representing the OR is replaced by a "voltage" source, A_{OR} , i.e., the affinity (or $-\Delta G_{OR}$, the Gibbs free energy change) of the OR. On the other hand, the branch voltage in electrical networks is equivalent to A_p ($A_p = -\Delta G_p$) i.e., the reaction step affinity.^{23,24,26} Figure 2, thus, represents the electrical analog for the HER/HOR mechanism, obtained directly from the RR graph in Fig. 1b. In doing this, the elementary steps are viewed as resistances, whereas the OR is viewed as a power source.³

Finally, to complete the electrical analogy, the step kinetics may also be cast in the form of Ohm's law.^{23,24,26} This step is not neces-

sary, of course, because Kirchhoff's laws apply for nonlinear elements, e.g., diodes as well but is intuitively appealing. It results from the following definitions for the net rate of a reaction step s_p and its affinity A_p ^{23,24,26}

$$r_p = \bar{r}_p - \tilde{r}_p \quad A_p = \frac{A_p}{RT} = \ln \frac{\bar{r}_p}{\tilde{r}_p} \quad (\rho = 1, 2, \dots, p) \quad [18]$$

The step resistance, R_p , is defined as the mean value of the $1/r_p$ between its limiting values, i.e., \bar{r}_p and \tilde{r}_p ²³

$$R_p = \frac{1}{\bar{r}_p - \tilde{r}_p} \int_{\tilde{r}_p}^{\bar{r}_p} \frac{1}{r_p} dr_p = \frac{\ln(\bar{r}_p/\tilde{r}_p)}{\bar{r}_p - \tilde{r}_p} = \frac{A_p}{r_p} \quad (\rho = 1, 2, \dots, p) \quad [19]$$

which, thus provides a linear relation between A_p and r_p , in the form of ohm's law. This, however, does not represent a linearization of kinetics but may be construed as simply the definition of step resistance, which clearly is not a constant but rather changes with reaction conditions, especially temperature and potential. Thus, using its definition $R_p = \ln(\bar{r}_p/\tilde{r}_p)/(\bar{r}_p - \tilde{r}_p)$, the step resistance may be calculated from step kinetics. The resistance remains unchanged whether a step is written for HOR or HER, i.e., whether the reaction is proceeding in the forward or reverse direction.

KPL.— The RR graph follows Kirchhoff's potential law (KPL),^{23,24,26} which for the g th FR is

$$\text{FR}_g: \sum_{\rho=1}^p \sigma_{g\rho} A_p = A_{OR} \quad \text{or} \quad \prod_{\text{FR}_g} K_p^{\sigma_{g\rho}} = K_{OR} \quad [20]$$

whereas for an ER

$$\text{ER}_g: \sum_{\rho=1}^p \sigma_{g\rho} A_p = 0 \quad \text{or} \quad \prod_{\text{ER}_g} K_p^{\sigma_{g\rho}} = 1 \quad [21]$$

where use has been made of Eq. 18, i.e., the De Donder relation, in obtaining the second set of relations.

Thus, KPL provides an important thermodynamic consistency check on the given kinetic parameters. For example, the KPL relation for ER₁, i.e., $A_V - A_H + A_T = 0$, implies, with the help of the relation $A_p/RT = \ln(\bar{r}_p/\tilde{r}_p)$

$$\left(\frac{\bar{r}_V}{\tilde{r}_V} \right) \left(\frac{\tilde{r}_H}{\bar{r}_H} \right) \left(\frac{\bar{r}_T}{\tilde{r}_T} \right) = 1 \quad \text{or} \quad \left(\frac{\tilde{\omega}_V}{\bar{\omega}_V} \right) \left(\frac{\bar{\omega}_H}{\tilde{\omega}_H} \right) \left(\frac{\bar{\omega}_T}{\tilde{\omega}_T} \right) = 1 \quad [22]$$

The calculated or experimentally determined rate constants must be consistent with these constraints. Alternatively, not all rate constants need to be predicted, some may be found from KPL relations. The affinities of the elementary reaction steps s_p in a FR are related to the OR affinity via a similar reaction, i.e. Eq. 20

$$A_{OR} = A_V + A_H = 2A_V + A_T = 2A_H - A_T \quad [23]$$

The data in Table II are, in fact, consistent with these two requirements.

Kirchhoff's Flux Law.— The Kirchhoff's flux law (KFL), analogous to the QSS analysis,^{12,36} applies at each node,^{23,24,26} i.e., $\sum_{\rho=1}^p m_{j\rho} r_p = 0$. Thus, at the IN

$$\text{IN}_1: (-2)r_T + (+1)r_V + (-1)r_H = 0 \quad [24]$$

The use of the step kinetics (Eq. 15) in this, thus, allows one to determine the unknown site fraction $\theta_{H,S}$ from

$$\underbrace{2(\tilde{\omega}_T - \bar{\omega}_T)\theta_{H,S}^2}_a + \underbrace{[4\tilde{\omega}_T + (\tilde{\omega}_V + \bar{\omega}_V) + (\tilde{\omega}_H + \bar{\omega}_H)]\theta_{H,S}}_b - \underbrace{(2\tilde{\omega}_T + \tilde{\omega}_V + \bar{\omega}_H)}_c = 0 \quad [25]$$

The solution to which is

$$\theta_{\text{H,S}} = \frac{1}{4(\tilde{\omega}_{\text{T}} - \tilde{\omega}_{\text{T}})} \left\{ - [4\tilde{\omega}_{\text{T}} + (\tilde{\omega}_{\text{V}} + \tilde{\omega}_{\text{V}}) + (\tilde{\omega}_{\text{H}} + \tilde{\omega}_{\text{H}})] + \sqrt{[4\tilde{\omega}_{\text{T}} + (\tilde{\omega}_{\text{V}} + \tilde{\omega}_{\text{V}}) + (\tilde{\omega}_{\text{H}} + \tilde{\omega}_{\text{H}})]^2 + 8(\tilde{\omega}_{\text{T}} - \tilde{\omega}_{\text{T}})(2\tilde{\omega}_{\text{T}} + \tilde{\omega}_{\text{V}} + \tilde{\omega}_{\text{H}})} \right\} \quad [26]$$

The other root of the quadratic equation does not provide a value between 0 and 1.³⁶ This may be used to obtain the surface coverage of adsorbed hydrogen for a given set of kinetic parameters, using which the step rates as well as step affinities and step resistances may be calculated.

The OR rate can next be calculated from the application of KFL at the TN, namely

$$\text{TN}_1: (-2)r_{\text{OR}} + (+1)r_{\text{V}} + (+1)r_{\text{H}} = 0 \quad [27]$$

Thus, although an explicit OR rate expression that contains all the three mechanistic steps cannot be obtained, numerical calculations of the OR rate can be readily performed for a variety of conditions, as shown in Fig. 3. Such QSS analysis is performed for the HOR/HER by many authors, for instance, by Gennero de Chialvo and Chialvo,^{12,36} although we interpret this as KFL applicable to the RR graph. Consequently, the results are similar.^{12,36}

One can similarly compute the QSS (KFL) rate for each of the individual limiting cases of the two-step mechanisms, namely, the Volmer–Heyrovsky, Volmer–Tafel, and Heyrovsky–Tafel mechanisms. Of course, the QSS (KFL) condition changes for each such limiting case, as does the dependence of $\theta_{\text{H,S}}$ on overpotential. Figure 3, thus, also provides QSS rates obtained numerically for each of the three two-step mechanisms. Figure 3 shows that the Heyrovsky–Tafel mechanism is not a significant contributor over any part of the range of overpotentials considered here for the alkaline system. In fact, even the Volmer–Heyrovsky and Volmer–Tafel mechanisms are individually applicable only in limited potential ranges.

A specific advantage of the RR graph approach, however, is that once the step rates, affinities, and resistances are hence obtained via KFL, a robust identification of the dominant reaction pathways may be accomplished based on a comparison of the flux (current) along different branches in the RR graph or via a comparison of pathway resistance. Moreover, comparison of resistance enables us to bottleneck the rate-limiting steps (RLS) without making any ad hoc assumptions, which in a sequence is defined as step(s) that contribute most significantly to the overall resistance of the sequence. In general, there can be more than a single RLS, the latter being distinct from the RDS. We previously presented such an analysis for the HER on Ni in alkaline electrolyte.³

However, the KFL/QSS approach discussed above is entirely numerical. We show next that, in fact, following the electrical analog of Ohm's law description of kinetics, an approximate, albeit accurate, explicit rate law for the general case involving all three steps can be obtained, as well as explicit rate expressions for limiting two-step mechanisms.

Ohm's Law Kinetics

The overall resistance of a reaction network may be calculated in terms of branch resistances using standard electrical circuit methods.⁴⁶ For the HOR/HER, the overall rate may be written as

$$2r_{\text{OR}} = \frac{A_{\text{OR}}}{R_{\text{OR}}} \quad [28]$$

where, for the circuit shown in Fig. 2, the overall resistance R_{OR} can be obtained by employing, e.g., a $\Delta - Y$ conversion utilized in electrical circuits.^{3,46} The rate r_{OR} on the left side of Eq. 28 has been doubled because the network involves the OR twice (Fig. 2). The overall network resistance for HOR/HER may be shown to be equal to

$$R_{\text{OR}} = \frac{R_{\text{T}}R_{\text{V}} + R_{\text{H}}(R_{\text{T}} + 4R_{\text{V}})}{2(R_{\text{T}} + R_{\text{V}} + R_{\text{H}})} \quad [29]$$

We have shown earlier that such a representation of the reaction rate is entirely consistent with the numerical results obtained from the conventional KFL/QSS analysis discussed in the last section.³ Unfortunately, the step resistances in Eq. 29 as defined above by Eq. 19 involve step kinetics including the activity of the intermediate species $\theta_{\text{H,S}}$, which is, of course, not known a priori, the determination of which is, in fact, the key goal of kinetic analysis. We have, thus, recently proposed an alternate Ohm's law representation of Eq. 28 of the form⁴⁷

$$2r_{\text{OR}} = \frac{E_{\text{OR}}}{R_{\text{OR}}^*} \quad [30]$$

in which the network resistance R_{OR}^* , of a form similar to Eq. 29 as described below, can, in fact, be determined a priori. Here, the thermodynamic driving force is defined as

$$E_{\text{OR}} \equiv 1 - z_{\text{OR}} \quad [31]$$

whereas the reversibility of the OR

$$z_{\text{OR}} = \tilde{r}_{\text{OR}}/\tilde{r}_{\text{OR}} = \exp(-A_{\text{OR}}) = \frac{1}{K_{\text{OR}}} \prod_{i=1}^n a_i^{v_i} \quad [32]$$

Furthermore, because this is a thermodynamic property using KPL, Eq. 20 for the A_{OR} , along with Eq. 18 for step affinities and the definition of step reversibility, $z_p = \tilde{r}_p/\tilde{r}_p = \exp(-A_p)$, we have

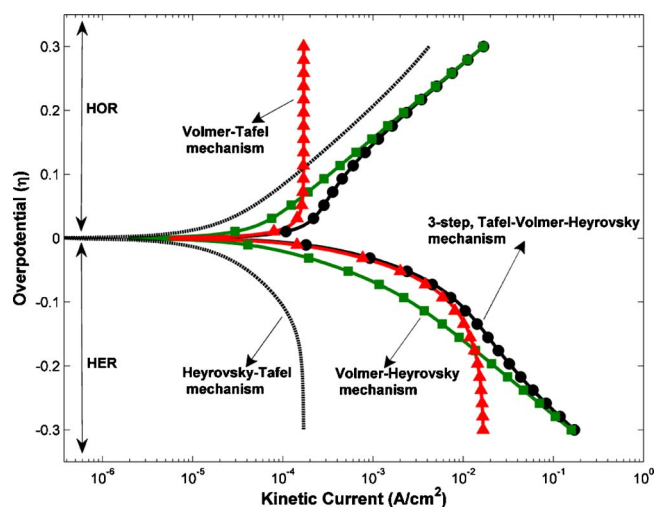


Figure 3. (Color online) Semilog plot of overpotential, η vs absolute value of kinetic current, i . Solid lines represent data obtained from solving QSS equation for the three-step Tafel–Volmer–Heyrovsky mechanism and each of the two-step mechanism, namely, Volmer–Heyrovsky, Volmer–Tafel, and Heyrovsky–Tafel mechanism, while symbols represent calculations from ohm's law. (●) Three-step mechanism Eq. 52, (■) two-step Volmer–Heyrovsky mechanism Eq. 59, (▲) two-step Volmer–Tafel mechanism Eq. 62.

$$z_{\text{OR}} = \prod_{\rho=1}^{q+1} (z_{\rho})^{\sigma_{\text{gp}}} = \prod_{\rho=1}^{q+1} \left(\frac{\tilde{r}_{\rho}}{\tilde{r}_{\rho}'} \right)^{\sigma_{\text{gp}}} \quad [33]$$

In fact, because the intermediate species get cancelled in an FR, there results

$$z_{\text{OR}} = \prod_{\rho=1}^{q+1} \left(\frac{\tilde{\omega}_{\rho}}{\tilde{\omega}_{\rho}'} \right)^{\sigma_{\text{gp}}} \quad [34]$$

i.e., it can be written in terms of the step weights and, hence, the OR reversibility, z_{OR} , is a known quantity for a given set of reaction conditions.

For the HOR, thus, for the different FRs (Eq. 3)

$$z_{\text{OR}} = \frac{\tilde{\omega}_{\text{V}} \tilde{\omega}_{\text{H}}}{\tilde{\omega}_{\text{V}}' \tilde{\omega}_{\text{H}}'} = \frac{\tilde{\omega}_{\text{V}}^2 \tilde{\omega}_{\text{T}}}{\tilde{\omega}_{\text{V}}'^2 \tilde{\omega}_{\text{T}}'} = \frac{\tilde{\omega}_{\text{H}}^2 \tilde{\omega}_{\text{T}}}{\tilde{\omega}_{\text{H}}'^2 \tilde{\omega}_{\text{T}}'} \quad [35]$$

The OR reversibility in the above relations may be written as follows by combining Eq. 16 with, e.g., the first of the relations in Eq. 35. Thus

$$z_{\text{OR}} = \left(\frac{\tilde{\omega}_{\text{V},0} \tilde{\omega}_{\text{H},0}}{\tilde{\omega}_{\text{V},0}' \tilde{\omega}_{\text{H},0}'} \right) e^{-4\psi} \quad [36]$$

When equilibrium is brought about by changing the hydrogen electrode overpotential to zero, i.e., as $\psi \rightarrow 0$, $z_{\text{OR}} \rightarrow 1$, and $R_{\rho} \rightarrow R_{\rho,0}$. Thus, the term in the parenthesis in the above expression must be unity, i.e., $\tilde{\omega}_{\text{V},0} \tilde{\omega}_{\text{H},0} = \tilde{\omega}_{\text{V},0}' \tilde{\omega}_{\text{H},0}'$, where these parameters in terms of rate constants at equilibrium potential and species concentrations are given in Eq. 13 and 17. The data in Table II indeed conform to this additional KPL relationship. The equation also explains the reciprocity in rate constants of the Volmer and Heyrovsky steps observed and commented on by Gennero de Chialvo and Chialvo.^{12,36} As a result, furthermore, the reversibility simply becomes

$$z_{\text{OR}} = e^{-4\psi} \quad [37]$$

It is, thus, clear from above that when $\psi > 0$, i.e., when the overpotential is positive, the OR proceeds as depicted in Eq. 1, i.e., as HOR. However, when $\psi < 0$, the OR is the HER. Further, at high overpotential in either direction, i.e., when $|\psi| \gg 0$, the reaction is essentially irreversible.

The above relation may alternately be obtained if either of the other two forms in Eq. 35 were used for this analysis, which further require $\tilde{\omega}_{\text{V},0}^2 \tilde{\omega}_{\text{T}} = \tilde{\omega}_{\text{V},0}'^2 \tilde{\omega}_{\text{T}}'$ and $\tilde{\omega}_{\text{H},0}^2 \tilde{\omega}_{\text{T}} = \tilde{\omega}_{\text{H},0}'^2 \tilde{\omega}_{\text{T}}'$ as additional KPL relations, which also the data in Table II agree with.

Further, using Eq. 30, 31, and 37 in $i = \nu_{\text{OR},e} F r_{\text{OR}}$, where $\nu_{\text{OR},e}$ is the stoichiometric coefficient of electrons in the overall electrode reaction (i.e., $\nu_{\text{OR},e} = +2$ for HOR and $\nu_{\text{OR},e} = -2$ for HER), and rearranging, the current density

$$i = \frac{\nu_{\text{OR},e} F (e^{2\psi} - e^{-2\psi})}{e^{2\psi} (2R_{\text{OR}}^*)} \quad [38]$$

This relation may alternately be expressed in terms of the exchange current density as follows. Thus, when equilibrium is brought about by changing the hydrogen electrode overpotential to zero, i.e., as $\psi \rightarrow 0$, then the net electrode current density $i \rightarrow 0$, but the current density in each direction \vec{i} and $\vec{i} \rightarrow i_0$. Of course, then the step resistance changes as well, $R_{\rho}^* \rightarrow R_{\rho,0}^*$, and the OR resistance changes concomitantly, $R_{\text{OR}}^* \rightarrow R_{\text{OR},0}^*$. Thus,

$$i_0 = \frac{|\nu_{\text{OR},e}| F}{2R_{\text{OR},0}^*} \quad [39]$$

and the current density then may be written in the alternate form

$$\frac{i}{i_0} = \frac{R_{\text{OR},0}^* (e^{2\psi} - e^{-2\psi})}{e^{2\psi} (R_{\text{OR}}^*)} \quad [40]$$

As mentioned above, R_{OR}^* in the above relations is the total network resistance, which may be written in terms of step resistance in the same form as Eq. 29, that is

$$R_{\text{OR}}^* = \frac{R_{\text{T}}^* R_{\text{V}}^* + R_{\text{H}}^* (R_{\text{T}}^* + 4R_{\text{V}}^*)}{2(R_{\text{T}}^* + R_{\text{V}}^* + R_{\text{H}}^*)} \quad [41]$$

where R_{ρ}^* is defined as the resistance of the step s_{ρ} when it is considered as the RDS, with all other steps at QE, i.e., $r_{\rho}^* = \tilde{r}_{\rho}^* (1 - z_{\text{OR}})$; when the entire affinity drop of the OR occurs across the RDS step, that of the QE steps approaches zero. Thus⁴⁷

$$R_{\rho}^* = \frac{1}{\tilde{r}_{\rho}^*} \quad [42]$$

The bullet in the superscript denotes the step as the RDS. Thus, r_{ρ}^* (\tilde{r}_{ρ}^*) is the rate (current) of the branch (resistor) s_{ρ} (R_{ρ}) if all other resistors in the circuit were short-circuited, i.e., if the entire motive force E_{OR} (A_{OR}) occurred across a chosen step (resistor) s_{ρ} (R_{ρ}), which, of course, would be the maximum step rate (current) in the step (resistor) for the given motive force.

By the same token, because the driving force (i.e., affinity, A_{ρ}) drop across the remaining steps is virtually zero, they may be considered to be at QE. The RDS and QE hypothesis (also called pseudo-equilibrium hypothesis) go hand in hand. It is thus, possible to explicitly determine R_{ρ}^* a priori following the LHHW algorithm.⁴⁷⁻⁴⁹

Equation 38, hence, provides an explicit rate expression for the QSS rate. We have shown before that this alternate form of Ohm's law kinetics provides exact results for the linear kinetics mechanisms (i.e., step kinetics linear in intermediates),⁴⁷⁻⁴⁹ whereas it provides an approximate, albeit, accurate results in other cases (i.e., when step kinetics are nonlinear in intermediates). Furthermore, Eq. 38 is in a form that is readily amenable to comprehension as well as pruning via comparison of resistances. We next show how to obtain the R_{ρ}^* employing the LHHW approach along with the notion of IRRs.

LHHW methodology for reaction resistance, R_{ρ}^ .*— Recall that an IRR, $\sum_{\text{IR}_k} \sigma_{\text{kj}} s_{\text{j}} = \text{IR}_k$, is an RR in which all intermediate species, except the given species I_k (along with a reference intermediate, say surface site, S), are eliminated, resulting in the $\text{IR}_k: \gamma_k I_k + (-\gamma_k) S + \sum_{i=1}^n (\gamma_{ki}) T_i = 0$. From KPL, the affinity of the IR_k , thus, is

$$\sum_{\text{IR}_k} \sigma_{\text{kj}} A_{\text{j}} = A_{\text{IR}_k} \quad [43]$$

Using the definition of step reversibility, as before, the IR reversibility

$$z_{\text{IR}_k} = \prod_{\text{IR}_k} (z_{\text{j}})^{\sigma_{\text{kj}}} = \prod_{\text{IR}_k} \left(\frac{\tilde{r}_{\text{j}}}{\tilde{r}_{\text{j}}'} \right)^{\sigma_{\text{kj}}} \quad [44]$$

Using in this the step kinetics in terms of step weights and noting that all intermediates but I_k and the vacant surface site S are eliminated by the stoichiometric numbers chosen to produce the IR

$$z_{\text{IR}_k} = \left(\frac{\theta_k}{\theta_0} \right)^{\gamma_k} \prod_{\text{IR}_k} \left(\frac{\tilde{\omega}_{\text{j}}}{\tilde{\omega}_{\text{j}}'} \right)^{\sigma_{\text{kj}}} \quad [45]$$

Further, if we select all the steps s_{j} in IRR, $\sum_{\text{IR}_k} \sigma_{\text{kj}} s_{\text{j}} = \text{IR}_k$, such that it does not include the step s_{ρ} under consideration as RDS or all the selected steps are among the QE steps, $z_{\text{IR}_k} = 1$, we have

$$\frac{\theta_{k,\rho}^*}{\theta_{0,\rho}^*} = \left[\prod_{\text{IR}_k} \left(\frac{\tilde{\omega}_{\text{j}}}{\tilde{\omega}_{\text{j}}'} \right)^{\sigma_{\text{kj}}} \right]^{1/\gamma_k} \quad [46]$$

We use the notation $\theta_{k,\rho}^*$ to represent site fraction of I_k when s_{ρ} is considered as the RDS. Finally, the site fractions thus calculated are used in the site balance, $1 = \sum_{k=0}^q \theta_{k,\rho}^*$, written in the form

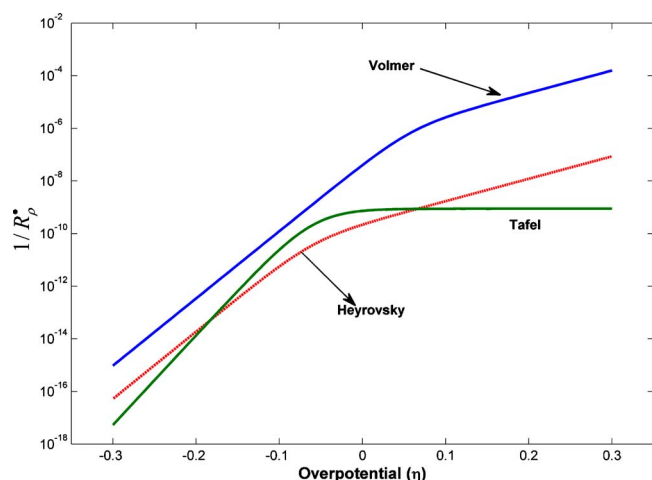


Figure 4. (Color online) Semilog plot of $1/R_p^*$ vs overpotential, η .

$$\frac{1}{\theta_{0,p}^*} = \sum_{k=0}^q \frac{\theta_{k,p}^*}{\theta_{0,p}^*} \quad [47]$$

Thus, the reference site fraction $\theta_{0,p}^*$, and, from it, all the remaining site fractions $\theta_{k,p}^*$ can be determined. As a result, the forward rate of s_p when it is considered as the RDS and, hence, the step resistance, R_p^* as per Eq. 42, can be evaluated a priori.

The general approach discussed above is utilized below for the specific case of HER/HOR mechanism here. Thus, with step s_T as the RDS

$$R_T^* = \frac{1}{\tilde{r}_T^*} = \frac{1}{\tilde{\omega}_T(\theta_{0,T}^*)^2} \quad [48]$$

The corresponding intermediate reaction for H·S is $\text{IR}_{\text{H}\cdot\text{S}} = (-1)s_V$. Using Eq. 46, we thus have $\theta_{\text{H}\cdot\text{S},\text{T}}^*/\theta_{0,\text{T}}^* = \tilde{\omega}_V/\tilde{\omega}_V$. Next from Eq. 47, $1/\theta_{0,\text{T}}^* = 1 + \tilde{\omega}_V/\tilde{\omega}_V$. Finally, using this in Eq. 48 along with Eq. 16

$$R_T^* = \frac{1}{\tilde{\omega}_T} \left(1 + \frac{\tilde{\omega}_V}{\tilde{\omega}_V} \right)^2 = \frac{1}{\tilde{\omega}_T} \left(1 + \frac{\tilde{\omega}_{\text{V},0}}{\tilde{\omega}_{\text{V},0}} e^{-2\psi} \right)^2 \quad [49]$$

Next, with step s_V as the RDS

$$R_V^* = \frac{1}{\tilde{r}_V^*} = \frac{1}{\tilde{\omega}_V \theta_{\text{H}\cdot\text{S},\text{V}}^*} = \frac{1}{\tilde{\omega}_V \left(\frac{\theta_{\text{H}\cdot\text{S},\text{V}}^*}{\theta_{0,\text{V}}^*} \right) \theta_{0,\text{V}}^*} \quad [50]$$

The corresponding intermediate reaction for H·S is $\text{IR}_{\text{H}\cdot\text{S}} = (+1)s_{\text{H}\cdot}$. Thus, $\theta_{\text{H}\cdot\text{S},\text{V}}^*/\theta_{0,\text{V}}^* = \tilde{\omega}_{\text{H}\cdot}/\tilde{\omega}_{\text{H}\cdot}$ along with $1/\theta_{0,\text{V}}^* = 1 + \tilde{\omega}_{\text{H}\cdot}/\tilde{\omega}_{\text{H}\cdot}$. Using the above in Eq. 50

$$R_V^* = \frac{1}{\tilde{\omega}_{\text{V},0} e^{\psi}} \left(1 + \frac{\tilde{\omega}_{\text{H}\cdot,0}}{\tilde{\omega}_{\text{H}\cdot,0}} e^{-2\psi} \right) \quad [51]$$

Similarly

$$R_{\text{H}\cdot}^* = \frac{1}{\tilde{r}_{\text{H}\cdot}^*} = \frac{1}{\tilde{\omega}_{\text{H}\cdot} \theta_{0,\text{H}\cdot}^*} = \frac{1}{\tilde{\omega}_{\text{H}\cdot,0} e^{\psi}} \left(1 + \frac{\tilde{\omega}_{\text{V},0}}{\tilde{\omega}_{\text{V},0}} e^{-2\psi} \right) \quad [52]$$

Figure 4 provides a plot of $1/R_p^*$ (maximum possible forward step rate) vs overpotential η . Based on Fig. 4, Volmer step seems to be the fastest over the entire range of overpotentials, whereas the resistances of the Heyrovsky and Tafel steps are of similar magnitude and may be rate-limiting over limited potential ranges, as discussed in more detail below. However, all three resistances are not of dramatically different magnitudes. Finally, the potential dependence of R_T^* is curious and explained by Eq. 49.

General Tafel–Volmer–Heyrovsky kinetics.— Assuming all three steps are significant, and combining Eq. 38 and 41

$$i = \frac{\nu_{\text{OR},e} F}{e^{2\psi}} \left\{ \frac{R_T^* + R_V^* + R_{\text{H}\cdot}^*}{R_T^* R_V^* + R_{\text{H}\cdot}^* (R_T^* + 4R_V^*)} \right\} (e^{2\psi} - e^{-2\psi}) \quad [53]$$

Using the step resistances obtained above in this and rearranging provides

$$i = \frac{(\nu_{\text{OR},e} F) \tilde{\omega}_T \tilde{\omega}_{\text{V},0}^2 \left[1 + \frac{\tilde{\omega}_{\text{H}\cdot,0}}{\tilde{\omega}_T \tilde{\omega}_{\text{V},0}} (\tilde{\omega}_{\text{V},0} e^{\psi} + \tilde{\omega}_{\text{V},0} e^{-\psi}) + \frac{(\tilde{\omega}_{\text{H}\cdot,0} e^{\psi} + \tilde{\omega}_{\text{H}\cdot,0} e^{-\psi})}{(\tilde{\omega}_{\text{V},0} e^{\psi} + \tilde{\omega}_{\text{V},0} e^{-\psi})} \right] (e^{2\psi} - e^{-2\psi})}{(\tilde{\omega}_{\text{V},0} e^{\psi} + \tilde{\omega}_{\text{V},0} e^{-\psi})^2 + (\tilde{\omega}_{\text{H}\cdot,0} e^{\psi} + \tilde{\omega}_{\text{H}\cdot,0} e^{-\psi}) \left[\frac{4\tilde{\omega}_T \tilde{\omega}_{\text{V},0}}{\tilde{\omega}_{\text{H}\cdot,0}} + (\tilde{\omega}_{\text{V},0} e^{\psi} + \tilde{\omega}_{\text{V},0} e^{-\psi}) \right]} \quad [54]$$

Although complex-looking, note that this is the first explicit expression available in the literature that provides the kinetics of the hydrogen electrode reaction in terms of the kinetics of all of the three accepted steps (Tafel–Volmer–Heyrovsky) considered together.

Further, when equilibrium is brought about by changing the hydrogen electrode overpotential to zero, i.e., as $\psi \rightarrow 0$, then the net electrode current density $i \rightarrow 0$, but the current density in each direction \vec{i} and $\tilde{i} \rightarrow i_0$. The above equation then provides the exchange current density

$$i_0 = \frac{|\nu_{\text{OR},e}| F \tilde{\omega}_T \tilde{\omega}_{\text{V},0}^2 \left[1 + \frac{\tilde{\omega}_{\text{H}\cdot,0}}{\tilde{\omega}_T \tilde{\omega}_{\text{V},0}} (\tilde{\omega}_{\text{V},0} + \tilde{\omega}_{\text{V},0}) + \frac{(\tilde{\omega}_{\text{H}\cdot,0} + \tilde{\omega}_{\text{H}\cdot,0})}{(\tilde{\omega}_{\text{V},0} + \tilde{\omega}_{\text{V},0})} \right]}{(\tilde{\omega}_{\text{V},0} + \tilde{\omega}_{\text{V},0})^2 + (\tilde{\omega}_{\text{H}\cdot,0} + \tilde{\omega}_{\text{H}\cdot,0}) \left[\frac{4\tilde{\omega}_T \tilde{\omega}_{\text{V},0}}{\tilde{\omega}_{\text{H}\cdot,0}} + (\tilde{\omega}_{\text{V},0} + \tilde{\omega}_{\text{V},0}) \right]} \quad [55]$$

For the kinetic data provided in Table II, this relation provides an exchange current density of $i_0 = 1.7 \times 10^{-4} \text{ A cm}^{-2}$ for HER on Pt in 0.5 M NaOH at $T = 296 \text{ K}$. This value compares well with that predicted using the correlation provided by Gennero de Chialvo and Chialvo³⁶ based on an extension of the Temkin development for a single RR. Many others have also suggested i_0 to be $\sim 10^{-4} \text{ A cm}^{-2}$ on Pt for alkaline electrolytes.^{21,50,51}

The last two expressions can be further combined to alternately express the current density in terms of exchange current density

$$i = i_0 \frac{\left\{ (\tilde{\omega}_{V,0} + \tilde{\omega}_{V,0})^2 + (\tilde{\omega}_{H,0} + \tilde{\omega}_{H,0}) \left[\frac{4\tilde{\omega}_T\tilde{\omega}_{V,0}}{\tilde{\omega}_{H,0}} + (\tilde{\omega}_{V,0} + \tilde{\omega}_{V,0}) \right] \right\} \left[1 + \frac{\tilde{\omega}_{H,0}}{\tilde{\omega}_T\tilde{\omega}_{V,0}} (\tilde{\omega}_{V,0}e^\psi + \tilde{\omega}_{V,0}e^{-\psi}) + \frac{(\tilde{\omega}_{H,0}e^\psi + \tilde{\omega}_{H,0}e^{-\psi})}{(\tilde{\omega}_{V,0}e^\psi + \tilde{\omega}_{V,0}e^{-\psi})} \right] (e^{2\psi} - e^{-2\psi})}{\left[1 + \frac{\tilde{\omega}_{H,0}}{\tilde{\omega}_T\tilde{\omega}_{V,0}} (\tilde{\omega}_{V,0} + \tilde{\omega}_{V,0}) + \frac{(\tilde{\omega}_{H,0} + \tilde{\omega}_{H,0})}{(\tilde{\omega}_{V,0} + \tilde{\omega}_{V,0})} \right] \left\{ (\tilde{\omega}_{V,0}e^\psi + \tilde{\omega}_{V,0}e^{-\psi})^2 + (\tilde{\omega}_{H,0}e^\psi + \tilde{\omega}_{H,0}e^{-\psi}) \left[\frac{4\tilde{\omega}_T\tilde{\omega}_{V,0}}{\tilde{\omega}_{H,0}} + (\tilde{\omega}_{V,0}e^\psi + \tilde{\omega}_{V,0}e^{-\psi}) \right] \right\}}$$
[56]

Although the above expressions are approximate, they are highly accurate as shown in comparison with the QSS numerical results over the entire range of potentials of interest for both HOR and HER, as shown in Fig. 3. Moreover, they quite nicely explain the asymmetry between the kinetics in the HER region vs that in the HOR region (Fig. 3).

Limiting Cases of Dual-Step Kinetics

When one of the two-step mechanisms (Volmer–Heyrovsky or Volmer–Tafel) is dominant, the third step may be removed from the RR graph and the corresponding simplified R_{OR}^* computed for the hence reduced circuit (Fig. 5). The Heyrovsky–Tafel mechanism is not considered here further based on the QSS results in Fig. 3. Thus, the overall resistances of the two-step pathways involved in HER/HOR are

$$\left. \begin{aligned} R_{VH}^* &= (R_V^* + R_H^*)/2 \\ R_{VT}^* &= 2R_V^* + R_T^*/2 \end{aligned} \right\} \quad [57]$$

which may be used for R_{OR}^* in Eq. 38–40, i.e., in $r_{OR} = E_{OR}/(2R_{OR}^*) \approx E_{OR}/(2R_{FR}^*)$.

Volmer–Heyrovsky mechanism.—For the Volmer–Heyrovsky mechanism, using the expressions for the Volmer and Heyrovsky resistances in Eq. 57 and rearranging

$$i_{VH} = \frac{\nu_{OR,e} F \tilde{\omega}_{V,0} \tilde{\omega}_{H,0} (e^{2\psi} - e^{-2\psi})}{(\tilde{\omega}_{H,0} + \tilde{\omega}_{V,0}) e^\psi + (\tilde{\omega}_{H,0} + \tilde{\omega}_{V,0}) e^{-\psi}} \quad [58]$$

This rate expression can, in fact, be derived via the KFL/QSS analysis as well, which provides an explicit solution in this case because the kinetics for both the Volmer and Heyrovsky steps are linear in the unknown surface intermediate concentration.

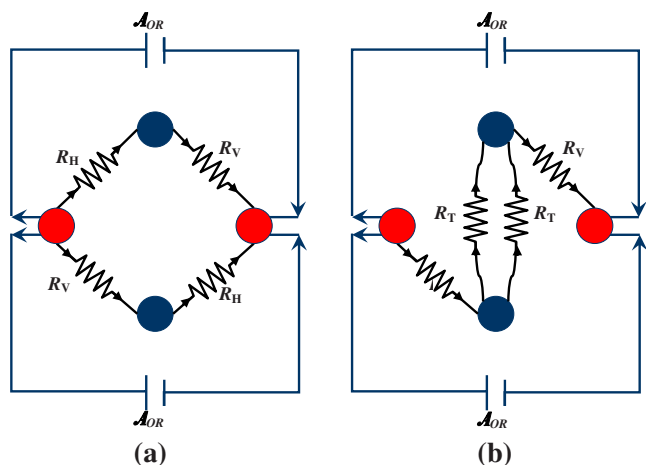


Figure 5. (Color online) Reduced RR circuit for (a) Volmer–Heyrovsky mechanism and (b) Volmer–Tafel mechanism.

The rate expression may further be written in an alternate form by using the identities, $e^\psi = \cosh \psi + \sinh \psi$, $e^{-\psi} = \cosh \psi - \sinh \psi$, and $\sinh(2\psi) = 2 \sinh \psi \cosh \psi$, and rearranging, to provide

$$i_{VH} = \frac{4\nu_{OR,e} F \left(\frac{\tilde{\omega}_{H,0}\tilde{\omega}_{V,0}}{\tilde{\omega}_{V,0} + \tilde{\omega}_{H,0}} \right) \sinh \psi}{2 - \left\{ 1 - \frac{(\tilde{\omega}_{V,0} + \tilde{\omega}_{H,0})}{(\tilde{\omega}_{V,0} + \tilde{\omega}_{H,0})} \right\} (1 - \tanh \psi)} \quad [59]$$

Further, the exchange current density from Eq. 39

$$i_{VH,0} = \frac{|\nu_{OR,e}| F \left(\frac{\tilde{\omega}_{V,0}\tilde{\omega}_{H,0}}{\tilde{\omega}_{V,0} + \tilde{\omega}_{H,0}} \right)}{1 + \frac{(\tilde{\omega}_{V,0} + \tilde{\omega}_{H,0})}{(\tilde{\omega}_{V,0} + \tilde{\omega}_{H,0})}} \quad [60]$$

Thus, an alternate form of the rate expression is obtained by combining the last two expressions

$$i_{VH} = \frac{4i_{VH,0} \left\{ 1 + \frac{(\tilde{\omega}_{V,0} + \tilde{\omega}_{H,0})}{(\tilde{\omega}_{V,0} + \tilde{\omega}_{H,0})} \right\} \sinh \psi}{2 - \left\{ 1 - \frac{(\tilde{\omega}_{V,0} + \tilde{\omega}_{H,0})}{(\tilde{\omega}_{V,0} + \tilde{\omega}_{H,0})} \right\} (1 - \tanh \psi)} \quad [61]$$

This is plotted in Fig. 3 for the HER/HOR in an alkaline system and is compared to the QSS result as well as the complete kinetic expression provided above. The expression is clearly adequate in the overpotential range of $-0.3 \text{ V} < \eta < -0.24 \text{ V}$ for HER and $0.13 \text{ V} < \eta < 0.3 \text{ V}$ for HOR in the alkaline system. Further, the asymmetry between the kinetics in the HER region vs that in the HOR region is a result of the coefficient of the tanh term in the denominator. For small ψ , this would be small, and the result would be a simple symmetric behavior as described by a Butler–Volmer kinetic expression.⁴⁴

Volmer–Tafel Mechanism.—For the Volmer–Tafel mechanism, using the expressions for the Volmer and Tafel resistances, along with $\tilde{\omega}_{V,0}\tilde{\omega}_{H,0} = \tilde{\omega}_{V,0}\tilde{\omega}_{H,0}$, and Eq. 57 in Eq. 39 and rearranging provides the exchange current density

$$i_{VT,0} = \frac{|\nu_{OR,e}| F (\tilde{\omega}_T \tilde{\omega}_{V,0}^2)}{(\tilde{\omega}_{V,0} + \tilde{\omega}_{V,0})^2 \left[1 + \frac{4\tilde{\omega}_T\tilde{\omega}_{V,0}}{\tilde{\omega}_{V,0}(\tilde{\omega}_{V,0} + \tilde{\omega}_{V,0})} \right]} \quad [62]$$

which may be combined with Eq. 40 to provide

$$i_{VT} = \frac{i_{VT,0} \left[1 + \frac{4\tilde{\omega}_T\tilde{\omega}_{V,0}}{\tilde{\omega}_{V,0}(\tilde{\omega}_{V,0} + \tilde{\omega}_{V,0})} \right] (e^{2\psi} - e^{-2\psi})}{\frac{1}{(\tilde{\omega}_{V,0} + \tilde{\omega}_{V,0})^2} \left[(\tilde{\omega}_{V,0}e^{\psi} + \tilde{\omega}_{V,0}e^{-\psi})^2 + \frac{4\tilde{\omega}_T\tilde{\omega}_{V,0}}{\tilde{\omega}_{V,0}} (\tilde{\omega}_{V,0}e^{\psi} + \tilde{\omega}_{V,0}e^{-\psi}) \right]} \quad [63]$$

which can alternately be written in terms of hyperbolic functions as above

$$i_{VT} = \frac{4i_{VT,0} \left[1 + \frac{4\tilde{\omega}_T\tilde{\omega}_{V,0}}{\tilde{\omega}_{V,0}(\tilde{\omega}_{V,0} + \tilde{\omega}_{V,0})} \right] \sinh \psi}{\cosh \psi \left[1 + \frac{(\tilde{\omega}_{V,0} - \tilde{\omega}_{V,0}) \tanh \psi}{(\tilde{\omega}_{V,0} + \tilde{\omega}_{V,0})} \right]^2 + \frac{4\tilde{\omega}_T\tilde{\omega}_{V,0}}{\tilde{\omega}_{V,0}(\tilde{\omega}_{V,0} + \tilde{\omega}_{V,0})} \left[1 - \frac{(\tilde{\omega}_{V,0} - \tilde{\omega}_{V,0}) \tanh \psi}{(\tilde{\omega}_{V,0} + \tilde{\omega}_{V,0})} \right]} \quad [64]$$

According to Fig. 3 based on this explicit rate expression, there is a great asymmetry in the Volmer–Tafel mechanism, described by the form of the denominator in the above expression. This mechanism is important for HER in an alkaline system in the overpotential range of $-0.1 \text{ V} < \eta < 0 \text{ V}$. For HOR in an alkaline system, the Volmer–Tafel mechanism is only applicable in a narrow overpotential range of $0 < \eta < 20 \text{ mV}$.

Note that this is the first such explicit expression for the Volmer–Tafel mechanism, as the corresponding QSS analysis cannot be written explicitly in such a form due to the nonlinearity of the kinetics. Thus, the QSS site coverage for the Volmer–Tafel kinetics is

$$\theta_{HS} = \frac{1}{4(\tilde{\omega}_T - \tilde{\omega}_T)} \{ [4\tilde{\omega}_T + (\tilde{\omega}_V + \tilde{\omega}_V)] - \sqrt{[4\tilde{\omega}_T + (\tilde{\omega}_V + \tilde{\omega}_V)]^2 - 8(\tilde{\omega}_T - \tilde{\omega}_T)(2\tilde{\omega}_T + \tilde{\omega}_V)} \} \quad [65]$$

which may be used in Eq. 15 for calculating the OR rate via the KFL/QSS approach.

Conclusions

The RR graph approach has been applied here to the hydrogen electrode reaction to obtain explicit rate expressions involving all three steps (Volmer–Heyrovsky–Tafel) as well as for more limiting two-step (Volmer–Heyrovsky and Volmer–Tafel) mechanisms. These expressions agree completely with the QSS analysis and nicely explain the asymmetry in current vs potential observed in the HER vs the HOR. Our topological approach is revealing and intuitive in depicting all possible reaction pathways as walks or paths on the RR graph and by visualizing the steps as resistances in an electrical circuit analog involving series and parallel pathways. Thus, the RR graph approach can be effectively used to identify the dominant reaction pathways. The approach further provides a link between the more rigorous but complex QSS kinetics and the LHHW analysis, which is simpler but arbitrary in its assumptions.

Thus, for the three-step hydrogen electrode reaction mechanism on Pt in 0.5 M NaOH at $T = 296 \text{ K}$, we find that the Volmer–Heyrovsky pathway is dominant in the potential region $-0.3 \text{ V} < \eta < -0.24 \text{ V}$ for HER and in the range $0.13 \text{ V} < \eta < 0.3 \text{ V}$ for HOR, whereas the Volmer–Tafel mechanism dominates in the potential region $-0.1 \text{ V} < \eta < 0 \text{ V}$ for HER and in $0 < \eta < 20 \text{ mV}$ for HOR. All three steps, however, need to be retained over the complete range of potentials of interest.

The above implications regarding the significance of the mechanism and kinetics of the HER reaction are limited to the three-step mechanism considered. Moreover, the conclusions are limited to a constant temperature of 298 K and liquid water (unit activity), corresponding to the given rate constants. However, the described approach is more general and can also be adapted to investigate additional steps in the mechanism when their kinetics as a function of temperature and potential become available. Further, of course, the

hydrogen electrode reaction in an acid electrolyte is also of great interest in connection with fuel cells and can also be analyzed via this approach.

Worcester Polytechnic Institute assisted in meeting the publication costs of this article.

List of Symbols

A_p	affinity of elementary reaction p
\mathbf{A}_p	dimensionless reaction affinity of elementary reaction p
E_p	activation energy for step s_p
F	Faraday's constant
ΔG_p	Gibbs free energy change of the elementary reaction p
$\Delta G_p^{\ddagger,0}$	Gibbs free energy of activation
h	Planck's constant
$\Delta H_p^{\ddagger,0}$	enthalpy of activation
I_p^*	maximum branch current
I_k	adsorbed intermediate species k
k_p	rate constant of the elementary reaction p
k_B	Boltzmann's constant
K_p	equilibrium constant of the elementary reaction p
m_{pj}	incidence coefficient
n	number of terminal species
p	number of elementary reactions
q	number of linearly independent intermediate species
r_p	net rate of the elementary reaction p
r_p^*	maximum rate of the elementary reaction p
\tilde{r}_p^*	maximum forward rate of the elementary reaction p
R	gas constant
R_p	resistance of elementary reaction p
R_p^*	resistance of elementary reaction s_p , when s_p is the RDS
s_p	elementary reaction p
$\Delta S_p^{\ddagger,0}$	entropy of activation
T	temperature, K
T_i	terminal species i
z_p	reversibility of reaction s_p

Greek

β_p	symmetry factor
γ_k	stoichiometric coefficient of intermediate species I_k in an intermediate reaction
γ_{ki}	stoichiometric coefficient of terminal species T_i in an intermediate reaction
η_p	electrode overpotential
θ_k	surface coverage of intermediate species k
$\theta_{k,p}^*$	surface coverage of intermediate species k when s_p is the RLS
Λ_p	pre-exponential factor
μ	number of linearly independent RRs
ν_i	stoichiometric coefficient of terminal species i in an OR
ρ	elementary reaction
σ_p	stoichiometric number for the elementary reaction p
Φ	electrode potential
Φ_0	equilibrium electrode potential
Φ_0^o	standard electrode potentials
ψ	dimensionless electrode overpotential, $0.5F\eta/RT$
ω_p	step weight for reaction s_p

References

1. J. M. Bockris and A. K. N. Reddy, *Modern Electrochemistry*, Plenum, New York (1973).
2. B. E. Conway and B. V. Tilak, *Electrochim. Acta*, **47**, 3571 (2002).
3. I. Fishtik, C. A. Callaghan, J. D. Fehribach, and R. Datta, *J. Electroanal. Chem.*, **576**, 57 (2005).
4. H. Kita, *J. Mol. Catal. A: Chem.*, **199**, 161 (2003).
5. P. M. Quaino, J. L. Fernandez, M. R. Gennero de Chialvo, and A. C. Chialvo, *J. Mol. Catal. A: Chem.*, **252**, 156 (2006).
6. P. M. Quaino, M. R. Gennero de Chialvo, and A. C. Chialvo, *Electrochim. Acta*, **52**, 7396 (2007).
7. J. X. Wang, T. E. Springer, and R. R. Adzic, *J. Electrochem. Soc.*, **153**, A1732 (2006).
8. C. A. Marozzi, M. R. Canto, V. Costanza, and A. C. Chialvo, *Electrochim. Acta*, **51**, 731 (2005).
9. Y. Ishikawa, J. J. Mateo, D. A. Tryk, and C. R. Cabrera, *J. Electroanal. Chem.*, **607**, 37 (2007).
10. A. B. Anderson, N. M. Neshev, R. A. Sidik, and P. Shiller, *Electrochim. Acta*, **47**, 2999 (2002).
11. Y. Cai and A. B. Anderson, *J. Phys. Chem. B*, **108**, 9829 (2004).
12. M. R. Gennero de Chialvo and A. C. Chialvo, *Phys. Chem. Chem. Phys.*, **3**, 3180 (2001).
13. J. K. Norskov, T. Bligaard, A. Logadottir, J. R. Kitchin, J. G. Chen, S. Pandalov, and U. Stimming, *J. Electrochem. Soc.*, **152**, J23 (2005).
14. W. Schmickler and S. Trasatti, *J. Electrochem. Soc.*, **153**, L31 (2006).
15. J. Meier, J. Schiøtz, P. Liu, J. K. Nørskov, and U. Stimming, *Chem. Phys. Lett.*, **390**, 440 (2004).
16. J. X. Wang, T. E. Springer, P. Liu, M. Shao, and R. R. Adzic, *J. Phys. Chem. C*, **111**, 12425 (2007).
17. B. E. Conway and L. Bai, *J. Electroanal. Chem. Interfacial Electrochem.*, **198**, 149 (1986).
18. N. Krstajic, M. Popovic, B. Grgur, M. Vojnovic, and D. Sepa, *J. Electroanal. Chem.*, **512**, 16 (2001).
19. N. Krstajic, M. Popovic, B. Grgur, M. Vojnovic, and D. Sepa, *J. Electroanal. Chem.*, **512**, 27 (2001).
20. R.-B. Lin and S.-M. Shih, *J. Chin. Inst. Chem. Eng.*, **39**, 475 (2008).
21. N. M. Markovića, S. T. Sarraf, H. A. Gasteiger, and P. N. J. Ross, *J. Chem. Soc., Faraday Trans.*, **92**, 3719 (1996).
22. K. C. Neyerlin, W. Gu, J. Jorne, and H. A. Gasteiger, *J. Electrochem. Soc.*, **154**, B631 (2007).
23. I. Fishtik, C. A. Callaghan, and R. Datta, *J. Phys. Chem. B*, **108**, 5671 (2004).
24. I. Fishtik, C. A. Callaghan, and R. Datta, *J. Phys. Chem. B*, **108**, 5683 (2004).
25. I. Fishtik, C. A. Callaghan, and R. Datta, in *Computational Material Science*, Vol. 15, J. Leszczynski, Editor, Elsevier, Amsterdam (2004).
26. I. Fishtik, C. A. Callaghan, and R. Datta, *J. Phys. Chem. B*, **109**, 2710 (2005).
27. S. A. Vilekar, I. Fishtik, and R. Datta, *J. Catal.*, **252**, 258 (2007).
28. O. A. Hougen and K. M. Watson, *Ind. Eng. Chem.*, **35**, 529 (1943).
29. J. A. Christiansen, *Adv. Catal.*, **5**, 311 (1953).
30. J. Horiuti, *Ann. N. Y. Acad. Sci.*, **213**, 5 (1973).
31. M. I. Temkin, *Adv. Catal.*, **28**, 173 (1979).
32. C. Wagner, *Adv. Catal.*, **21**, 323 (1970).
33. J. Tafel, *Z. Phys. Chem.*, **50**, 641 (1905).
34. J. Heyrovsky, *Recl. Trav. Chim. Pays-Bas*, **46**, 582 (1927).
35. T. Volmer and M. Erdey-Gruz, *Z. Phys. Chem. Abt. A*, **150**, 203 (1930).
36. M. R. Gennero de Chialvo and A. C. Chialvo, *J. Electrochem. Soc.*, **147**, 1619 (2000).
37. S. Völkening, K. Bedürftig, K. Jacobi, J. Winterlin, and G. Ertl, *Phys. Rev. Lett.*, **83**, 2672 (1999).
38. K. Bedürftig, S. Völkening, Y. Wang, J. Winterlin, K. Jacobi, and G. Ertl, *J. Chem. Phys.*, **111**, 11147 (1999).
39. J. Rossmeisl, J. K. Nørskov, C. D. Taylor, M. J. Janik, and M. Neurock, *J. Phys. Chem. B*, **110**, 21833 (2006).
40. I. Fishtik and R. Datta, *Stud. Surf. Sci. Catal.*, **133**, 123 (2001).
41. I. Fishtik and R. Datta, *Ind. Eng. Chem. Res.*, **40**, 2416 (2001).
42. P. C. Milner, *J. Electrochem. Soc.*, **111**, 228 (1964).
43. J. Happel and P. H. Sellers, *Adv. Catal.*, **32**, 273 (1983).
44. T. Thampam, S. Malhotra, J. Zhang, and R. Datta, *Catal. Today*, **67**, 15 (2001).
45. L. Bai, *J. Electroanal. Chem.*, **355**, 37 (1993).
46. N. Balabanian and T. Bickart, *Electrical Network Theory*, John Wiley & Sons, New York (1969).
47. S. A. Vilekar, I. Fishtik, and R. Datta, *Chem. Eng. Sci.*, **64**, 1968 (2009).
48. S. A. Vilekar, I. Fishtik, and R. Datta, in *Silica and Silicates in Modern Catalysis*, I. Halasz, Editor, p. 49, Transworld Research Network, Kerala, India (2010).
49. S. A. Vilekar, I. Fishtik, and R. Datta, *Chem. Eng. Sci.*, **65**, 2921 (2010).
50. V. S. Bagotzky and V. Osterova, *J. Electroanal. Chem. Interfacial Electrochem.*, **43**, 233 (1973).
51. K. Machida and M. Enyo, *Bull. Chem. Soc. Jpn.*, **59**, 725 (1986).